Local Cluster Distortions in Amorphous Organotin Sulfide Compounds and Their Influence on the Nonlinear Optical Properties

Jens R. Stellhorn, Shinjiro Hayakawa, Benjamin D. Klee, Benedict Paulus, Jonathan Link Vasco, Niklas Rinn, Irán Rojas León, Christopher A. Hosier, Stefanie Dehnen, and Wolf-Christian Pilgrim*

The local structure of four amorphous organotin sulfide compounds is investigated by X-ray absorption spectroscopy. These compounds exhibit a nonlinear optical (NLO) response upon irradiation with a continuous-wave near-infrared laser. Their basic structural motif is a hetero-adamantane cluster with different organic substituent, but depending on the morphology of the compound and the choice of the organic substituent, the nature of the NLO response changes to either a second harmonic generation or the generation of a supercontinuum, potentially appearing as white light. The structural results provide an experimental evidence that the nature of the NLO properties is tied to distortions occurring at the cluster core, with almost ideal clusters in compounds that show second harmonic generation, and strongly distorted clusters in the case of compounds that generate a supercontinuum. These distortions may enable a closer proximity of the cluster cores, altering the intermolecular order, and thereby influencing the NLO response.

J. R. Stellhorn, S. Hayakawa
Department of Applied Chemistry
Hiroshima University
Hiroshima 739-8527, Japan
E-mail: stellhoj@hiroshima-u.ac.jp
J. R. Stellhorn, B. D. Klee, B. Paulus, J. Link Vasco, N. Rinn, I. Rojas León, C. A. Hosier, S. Dehnen, W.-C. Pilgrim
Department of Chemistry
Philipps University Marburg
35032 Marburg, Germany
J. R. Stellhorn
Department of Physics
Nagoya University
Nagoya 464-0862, Japan
B. D. Klee
Complex Fluid Research Department
Wigner Research Centre for Physics
Budapest 1121, Hungary
N. Rinn, I. Rojas León, S. Dehnen
Karlsruhe Institute of Technology (KIT)
Institute of Nanotechnology (INT)
76344 Eggenstein-Leopoldshafen, Germany

1. Introduction

Heteroadamantane cluster compounds of the composition $[(RSn)_4S_6]$ (R = organic side group) were recently found to exhibit strong nonlinear optical (NLO) properties, setting off a discussion about their potential use as cheap and efficient warm-white light emitters when driven by a low-power continuous-wave infrared laser diode.[1–4] This so-called white-light generation (WLG) is the common denomination of a physical phenomenon referred to as supercontinuum generation, that is, the extreme spectral broadening of a light source propagating through a nonlinear medium.[5,6] WLG was demonstrated for amorphous $[(RSn)_4S_6]$ compounds with electron-rich organic substituents, like phenyl (Ph), η^1-cyclopentadienyl (η^1-Cp),[7–9] or benzyl.[8] On the other hand, a variation of the organic side group can change the NLO response, leading instead to a strong second harmonic generation (SHG) in (amorphous) compounds with R = methyl (Me) or naphthyl (Np).[2]

Some of these compounds can also be prepared in a crystalline form, in which only SHG was detected so far. Therefore, it was suggested that the nature of the NLO effect is closely linked to the existence of long- or intermediate-range atomic order.

Density functional theory (DFT) calculations of isolated molecules indicate that these compounds consist of $\{Sn_4S_6\}$ cluster cores in a hetero-adamantane configuration, with the organic substituents chemically bound to Sn.[8] (An illustration of the cluster geometry is included in **Figure 1**.) The most recent DFT study[10] provides evidence that the relative orientation of neighboring clusters can significantly affect the nature of the NLO effect. In the Ph-substituted compound, a predominance of the relatively isotropic core–core interactions counterbalance the rather directional interactions involving the organic substituents, leading to a lower degree of order (as compared e.g., to the Np-substituted compound). It is especially noteworthy that the clusters can come into very close proximity even in the simulation of a relatively simple dimer system. There, the distance between two S atoms of neighboring clusters can actually be shorter than the intra-molecular S–S separation.

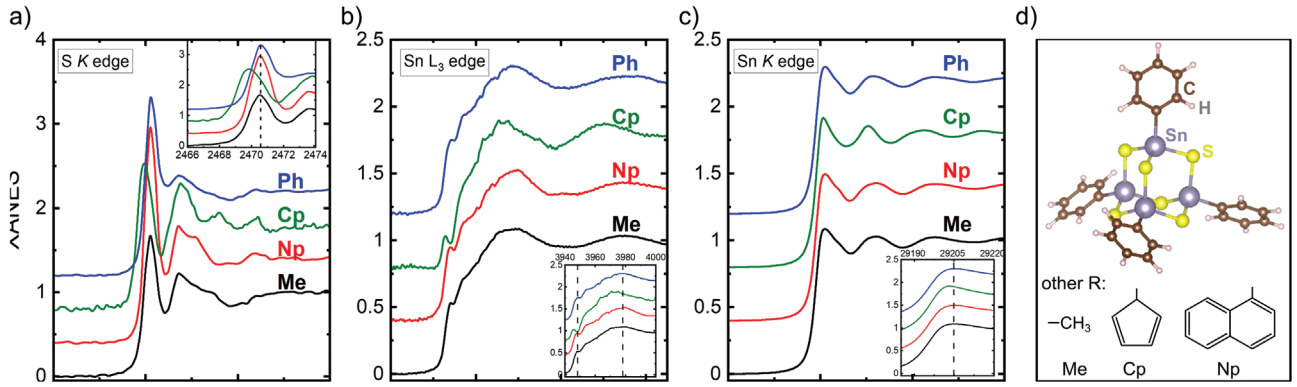

Figure 1. XANES data for the four organotin sulfide samples (Me: black, Np: red, η^1-Cp: green, Ph: blue, shifted upward for clarity) a) at the S *K* edge, b) at the Sn L_3 edge, and c) at the Sn *K* edge. The insets highlight the regions close to the first maxima of the respective edges. A model of the $[(PhSn)_4S_6]$ cluster from a DFT simulation[1] is illustrated in (d), along with schematic illustrations of the other organic substituents.

A recent study[11] based on X-ray scattering as well as extended X-ray absorption fine structure spectroscopy (EXAFS) data and a reverse Monte Carlo (RMC) modeling procedure,[12,13] investigated the local structure of the $[(PhSn)_4S_6]$ compound, which was one of the first examples of this class of compounds exhibiting WLG.[2] Substantial distortions of the heteroadamantane cluster cores were found, which were identified as being responsible for the tendency of the molecules to suppress crystal formation, and are therefore an important feature of the WLG effect. Moreover, the emerging view is that these findings can be generalized also to other such heteroadamantane-derived clusters with different organic substituents.[14,15]

However, the exact extent of these distortion is still unclear, as well as their relationship with the different NLO responses for different substituents. To solve this issue and to gain a deeper insight into the local structure of these clusters, we performed X-ray absorption spectroscopy measurements at the absorption edges of both S and Sn in a series of $[(RSn)_4S_6]$ compounds, providing an ample experimental basis of the actual atomic structure. The distance range covered by EXAFS measurements in amorphous compounds is generally limited to the nearest and next-nearest atomic neighbors, rendering a thorough characterization of the entire inter-molecular order extremely difficult. (Some details on EXAFS characterizations for organic–inorganic hybrid amorphous materials are presented in ref. [16].) On the other hand, since our previous studies[10,11,15] suggest that the inter-cluster distances may be on the same length scale as (or even smaller than) the intra-cluster atomic pairs, they fall in the reliable range probed of this method, as do the local distortions of the cluster cores. Therefore, the measurements presented here provide a valuable contribution to the as of yet puzzling physical mechanisms behind the different NLO effects.

2. Results

In the following, we compare the experimental results for four samples of the general composition $[(RSn)_4S_6]$ with the organic side groups R being methyl (Me), naphthyl (Np), η^1-cyclopentadienyl (η^1-Cp), and phenyl (Ph), all of which are in an overall amorphous state. These compounds show exhibit different NLO response as described in the introduction, with Me- and Np-substituents leading to SHG, while Ph-substituents (and conditionally η^1-Cp, see above) lead to WLG. See the Experimental Section for further details.

A first insight into the atomic arrangements and chemical bonds is accessible directly from the near-edge part of the absorption spectrum (XANES). The spectra are displayed in Figure 1 for the S *K* (a), Sn L_3 (b), and Sn *K* (c) edges. The spectra in general exhibit a two-signal structure at the S *K* edge (the second main signal is diminished for R = Ph), and a pre-edge shoulder before the main peak at the Sn L_3 edge (marked as vertical dashed lines in the inset). At the Sn *K* edge (c), the spectra exhibit smooth edge steps and resemble each other in appearance. At first glance, a striking exception in the series of datasets is the cluster with η^1-Cp substituents: as highlighted in the insets in Figure 1, all maxima of the XANES signals of this sample are shifted to lower energies: by 0.8 eV (S *K* edge), 3.5 eV (Sn L_3), and 2.2 eV (Sn *K*), respectively. Furthermore, the structure of the signal is also considerably different from the other samples, with a sharper second peak in the Sn *K* XANES and a smaller pre-dge peak in the Sn L_3 XANES. This observation already indicates a substantial difference in the electronic configuration of the Sn atoms in the $[(\eta^1\text{-CpSn})_4S_6]$ cluster. We note that the XANES shifts are also reproduced by simulations from the DFT results.[14] Furthermore, in the S XANES data, the structure of the signals of both the clusters with Ph- and η^1-Cp-substituents differs from the other samples. This further suggests a structural distinction between the Ph- and η^1-Cp- versus the Me- and Np-substituted clusters.

The EXAFS data are illustrated in **Figure 2** as Fourier transform magnitudes for all four systems, along with the best fits from the "single cluster fitting" approach. For the Sn *K* edge, only the data at 34 K are shown; the full set of data and fits (room temperature measurements) as well as the functions in *k*-space can be found in Figures S1–S4, Supporting Information. The main signals of these datasets, appearing around 2 Å, correspond to the Sn–S scattering paths (and S–Sn, respectively). It is found that the Sn *K* EXAFS data in general can be fitted reasonably well with the single cluster model. This is also true for the S *K* EXAFS data of the clusters with R = Me and

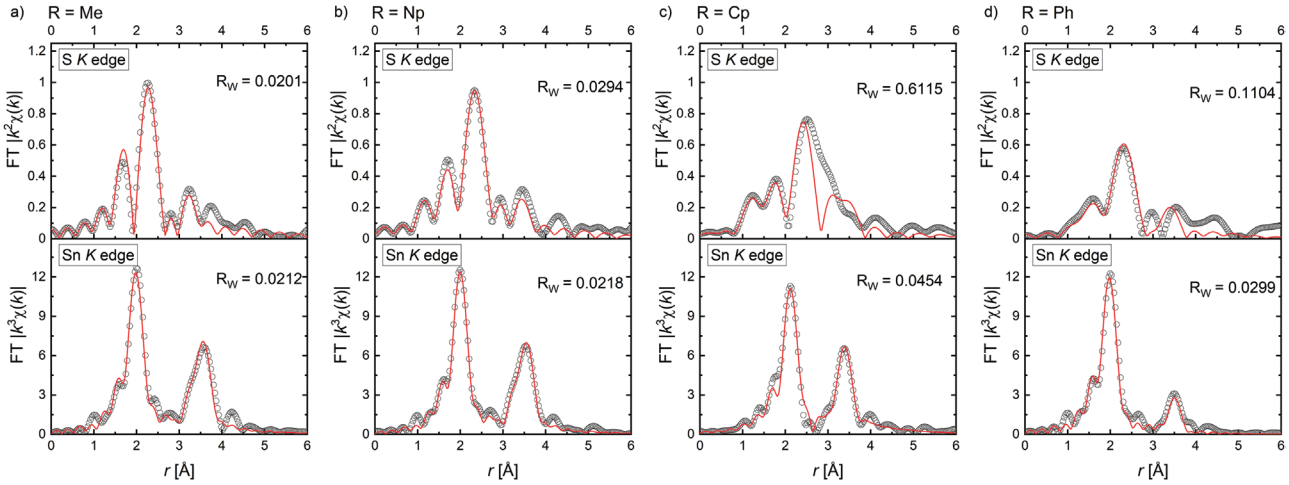

Figure 2. Experimental data and fits from single molecule models in *R* space, for the a) methyl-, b) naphthyl-, c) η^1-cyclopentadienyl- and d) phenyl-substituted samples. Shown here are the Fourier transform magnitudes of the EXAFS functions with appropriate *k*-weighting, for the S *K* as well as for the Sn *K* edge data. Fit qualities are noted with the goodness-of-fit parameters R_w. Note that the fits for both S *K* and Sn *K* data result from the same model.

Np (a,b), but not for R = η^1-Cp and Ph (c,d). In the latter group, it is clearly necessary to consider an additional scattering path in the second neighbor region (around 2.6–4 Å). This is also represented by the relatively poor quality of the goodness-of-fit parameters R_w for the η^1-Cp- and Ph-clusters (values are given in the figure).

The fit results for the interatomic distances are illustrated in **Figure 3**, along with the reference values from DFT simulation of the isolated clusters[1] (dashed lines). The individual coordination shells of the different correlations Sn–C, Sn–S, Sn–Sn, and S–S (with increasing distance) can be clearly distinguished. Concerning the local atomic environment of the tin atoms, the interatomic distances for the clusters with Me- and Np-substituents are all around 0.02–0.06 Å shorter than the reference values. This is still a remarkably good agreement considering that the reference values are determined for an isolated molecule, whereas the experimental data represent the situation of the structure in the amorphous phase, in which the clusters are packed relatively tightly.[17,18]

A clear distortion of the cluster is observed for R = η^1-Cp, with an elongation of the Sn–C and Sn–S bond to 2.23(2) and 2.51(1) Å, respectively, and a contraction of the Sn–Sn distance to 3.60(2) Å. For the [$(PhSn)_4S_6$] cluster, the Sn–Sn distance with 3.74(2) Å is also significantly shorter than for the clusters with Me- and Np-substituents (3.81(1) and 3.82(1) Å, respectively).

The intramolecular S–S distances all are significantly shorter than the reference values by about 0.2 Å, though it has to be noted that the error bars are relatively large in the fits from the S *K* EXAFS data due to the small accessible *k*-range.

The corresponding mean square relative displacement (MSRD) factors are illustrated in **Figure 4** for the Sn *K* EXAFS data at 34 K. The Sn–C and Sn–S MSRD are overall close to 0.003 Å^2. However, the Sn–Sn displacements exhibit a clear distinction, with small values for the Me- and Np-substituted clusters, and significantly higher values for clusters with R = η^1-Cp and Ph (0.004 and 0.009 Å^2, respectively).

To improve the "single molecule fit model" for the [$(\eta^1$-$CpSn)_4S_6$] and [$(PhSn)_4S_6$] clusters, we consider additional paths for the EXAFS fits. Since the Sn *K* data already exhibit reasonable goodness-of-fit values R_w (see Figure 2), it stands to reason that the missing paths are mostly S-based correlations, presumably S–S. Therefore, we added another path S–$S_{additional}$ at an intermediate range around 3.6 Å, with the distance as well as the coordination number as free parameters. The resulting

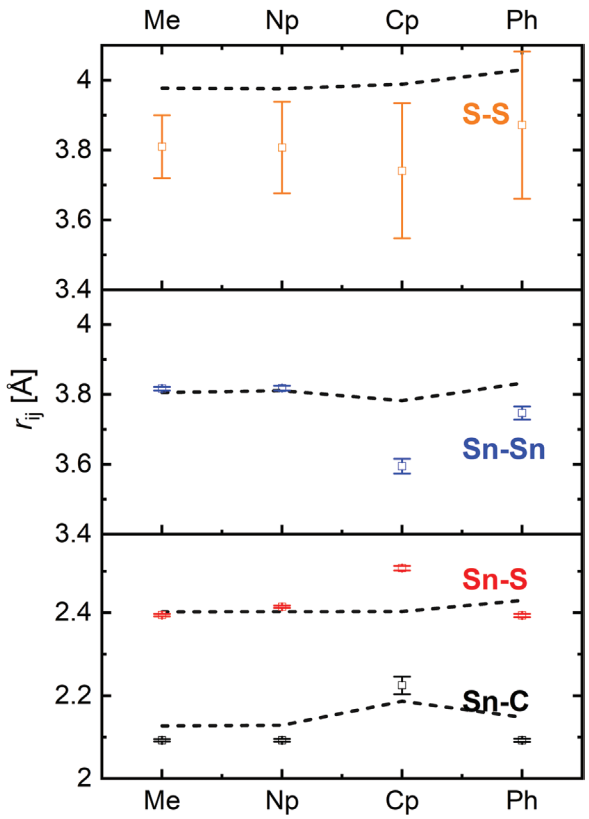

Figure 3. Fit results for the distances of the different paths from the single molecule fits with error bars. The dashed lines indicate the reference values from DFT simulations.[1]

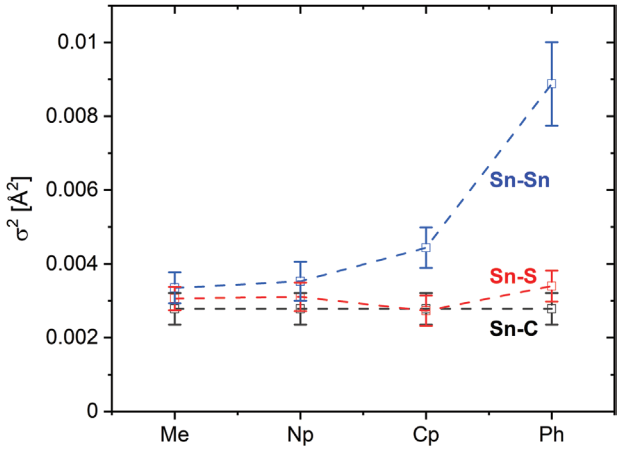

Figure 4. Fit results for the EXAFS mean displacements σ^2 for the single molecule fits of the Sn *K* EXAFS data at 34 K.

fitting curves as well as the result for the distance parameters are displayed in **Figure 5**. The inter-molecular S–S coordination numbers were determined to be around 1. As illustrated in the figure, the fitting qualities can be strongly improved by this approach.

3. Discussion

The additional S–S paths (S–$S_{additional}$) used in the models in Figure 5 can be interpreted either as part of the distortion of the cluster core (i.e., a range of different S–S distances are realized) or as inter-molecular interactions (or a mix of both effects). There are persuasive arguments for both views: the cluster dimers studied by DFT simulations[10] show that inter-molecular S–S distances should appear in the range 3.5–3.7 Å, depending on the dimer geometry (stacked vs alternating arrangements of the substituents). On the other hand, our recent RMC study on $[(PhSn)_4S_6]$ clusters[11] finds substantial cluster core distortions,

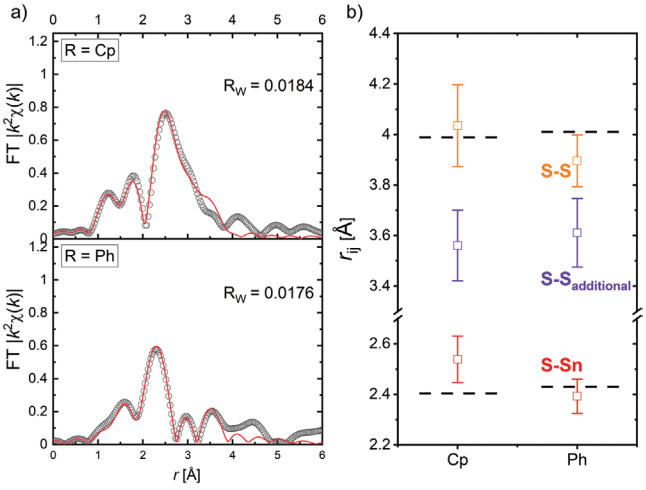

Figure 5. Fits from models with an additional S–S path, and resulting distance parameters. Dashed lines again indicate the results from DFT simulations of isolated clusters.

with S–S distances varying broadly between 3.5-4.2 Å (in addition to inter-molecular S–S distances also found in the same range).

Based on the structural parameters determined by the EXAFS fitting models (Figures 3 and 5), the samples can be categorized in two groups: i) clusters with Me- and Np-substituents can be fitted as single molecules, whereas ii) clusters with R = η^1-Cp and Ph are distorted and possess additional S–S bonds. Since the materials in these groups also differ in the nature of their NLO properties, with SHG for group (i) and WLG for group (ii), it is plausible to consider these as characteristic structure–property relationships.

Concerning group (i), that is, Me- and Np-substituted clusters, the $\{Sn_4S_6\}$ cores generally remain in their ideal adamantane-like geometry, as indicated by the similar distance parameters and the small MSRD's (Figures 3 and 4). A notable disparity from the DFT model is only found for the S–S distance, which indicates a certain flexibility of the Sn–S–Sn bond angle of the hetero-adamantane cage. Furthermore, no appreciable inter-molecular interactions (which should be visible as S–$S_{additional}$) can be observed. This does not mean that there is no inter-molecular order—indeed, a certain degree of intermediate-range order is regarded as a requirement for SHG, since it allows for phase-matching conditions.[2,10] However, the cluster cores do not approach each other in the range up to about 4 Å, which is the effective range of view of the EXAFS data. It is rather suggested that the inter-molecular ordering is achieved by the substituents, for example, in the case of R = Np by the dispersive interactions between the extended π systems. This effect was quantified in a previous study by a decomposition of the cluster dimer binding energies, showing a much stronger substituent–substituent interaction for Np- than for Ph-substituted clusters.[10] In contrast, the ordering of the $[(MeSn)_4S_6]$ clusters was explained by the low steric demand and the low flexibility of the ligand.[2] This is confirmed by the fact that these clusters can even form single crystals.[19] As a result, the cluster cores do not come into close proximity with each other, which is in agreement with the presented experimental data.

On the other hand, major distortions are observed for the cluster cores in the compounds which generally show WLG, that is, clusters with R = η^1-Cp and Ph. These distortions are realized in different manners: in the $[(\eta^1\text{-}CpSn)_4S_6]$ clusters, all interatomic distances differ largely from the ideal adamantane-like cage structure. Here, it is worth noting again that the shift of the XANES signal to lower energies in both S and Sn (Figure 1) indicates a lower oxidation state of both elements as compared to the situation in the other clusters. This process leads to an overall destabilization of the cluster core, which facilitates the destruction of the cluster during an optical measurement, as described in the introduction. Presumably, this is related to the electron-rich, but non-aromatic, η^1-Cp substituent, that transfers electron density into the cluster core. This interpretation is substantiated by the agreement between the experimental and simulated XANES signals (illustrated in ref. [14]).

In contrast, in the $[(PhSn)_4S_6]$ cluster, a deviation from the ideal cluster geometry is not evident at the level of chemical bonds, but is rather found on the next-nearest neighbor level, realized as contracted Sn–Sn distances (Figure 3) with large mean displacements (Figure 4). This indicates a considerable flexibility of the bond angles of the $[Sn_4S_6]$ cluster core.

With respect to the theoretical study by Hanau et al.,[10] it may be argued that the dispersive interactions between the Ph-substituents are too weak to prevent close contacts between the clusters. This results in an increased core–core interaction, which are not strong enough to significantly affect the Sn–S chemical bond length, but can induce distortions on the second-neighbor level (the bond angles). Consequently, the cluster distortions in both η^1-Cp- and Ph-substituted clusters increase the variety of possible cluster–cluster approach geometries, thereby increasing molecular disorder and smearing out the electronic interactions to such a degree that the NLO characteristics change from SHG to WLG.

4. Conclusion

The local structure of four amorphous organotin sulfide compounds with R = Me, Np, η^1-Cp, and Ph was investigated experimentally by XANES and EXAFS measurements. The basic structural motif of hetero-adamantane clusters is confirmed for all samples. However, the different nature of their nonlinear optical properties (SHG vs WLG) is correlated with distortions of the cluster cores and/or intermolecular core–core interactions: clusters with Me- and Np-substituents, exhibiting second harmonic generation, remain in their almost ideal cluster geometry, while Ph- and η^1-Cp-substituted clusters, exhibiting white-light generation, are strongly distorted. The distortions are realized in different manners, with a significant change of the Sn–S chemical bonds in the $[(\eta^1\text{-CpSn})_4S_6]$ clusters, and large mean square relative displacements in the $[(PhSn)_4S_6]$ clusters. Both facilitate a closer proximity of the cluster cores, strongly affecting the intermolecular order and, in turn, influencing the NLO response. Our study presents a deeper level of understanding regarding the structure–property relationships in this new class of efficient nonlinear optical materials, thus outlining a path for the future direction of research in this area.

5. Experimental Section

Synthesis: Four different samples of the general composition $[(RSn)_4S_6]$ were prepared with the organic side groups R being methyl (Me), naphthyl (Np), η^1-cyclopentadienyl (η^1-Cp), and phenyl (Ph). The samples were prepared by reaction of R-$SnCl_3$ with Na_2S in toluene, and were obtained as overall amorphous powders. More details of the sample preparation are given elsewhere.[1,8] The samples used for the X-ray spectroscopy experiments in this study were prepared via the same synthesis route and in the same laboratory as in the indicated references, which implied comparable powder gradations and morphology.

X-Ray Absorption Spectroscopy Experiments: The S *K* extended X-ray absorption fine structure (EXAFS) (2.47 keV) and the Sn L_3 near-edge structure (XANES) (3.93 keV) spectroscopy experiments were conducted at BL11 of the Hiroshima Synchrotron Radiation Center (HSRC), Hiroshima University, Higashi-Hiroshima, Japan. This beamline was designed to maximize the beam intensity on the sample in the 2–5 keV region by forgoing the use of Be windows and minimizing air paths.[20]

The synchrotron radiation from a bending magnet was monochromatized with a Si(111) double-crystal monochromator. A Ni-coated pre-mirror system was utilized to reject higher harmonics. To detect the incident flux, a commercial ionization chamber filled with a N_2/He (20:80) mixture was placed between the end of the beamline and the sample chamber. The beam size (FWHM) at the sample position was ≈3 mm × 1 mm. The sample chamber was filled with He to reduce air absorption. The transmitted beam was detected by another ionization chamber filled with air, while the fluorescence intensity was measured with a Si drift detector (SDD). For the sample preparation, a fine layer of the sample (about 1–2 mg in an area of 1 cm^2, corresponding to about 1.5 absorption lengths) was placed between two thin polypropylene films (6 µm thickness), and was oriented with a 45° angle to the beam, to allow for the simultaneous measurement of transmission and fluorescence intensity.

Additionally, high-energy EXAFS measurements at the Sn *K* edge (29.20 keV) were performed at the beamline P65 of the PETRA III ring (Hamburg, Germany).[21] Experiments were performed in transmission mode at room temperature (RT) and at $T = 34$ K. For these measurements, the samples were mixed with graphite and pressed to pellets with thicknesses corresponding to 2 absorption lengths.

Data Analysis: The EXAFS data were analyzed with the DEMETER program package.[22] For modeling the EXAFS data, the three datasets (S *K* EXAFS at RT, Sn *K* EXAFS at RT and at 34 K) were fitted simultaneously. The initial model for the fit was a cluster model obtained from an ab initio simulation of the corresponding $[(RSn)_4S_6]$ cluster.[1,10] Two subsequent approaches were pursued for the data fitting procedure:

1) In the first model, only scattering paths within a single $[(RSn)_4S_6]$ cluster were used, which were Sn–C, Sn–S, and Sn–Sn for the Sn *K* EXAFS data, and for the S *K* EXAFS data these were S–Sn and S–S. The bond distance parameters for Sn–S and S–Sn were correlated between the Sn *K* and S *K* datasets. (Note that in this nomenclature for the scattering paths, the first element denotes the emitter atom, i.e., the "Sn–S" path is related to the Sn *K* edge data, while "S–Sn" is related to the S *K* edge data.) Fit windows were defined between 1.2–4.0 Å for the Sn *K* data, and between 1.5–3.8 Å for the S *K* data. MSRD factors σ^2 were also fitted for each path. For the S-based EXAFS, the uncertainties in these factors were quite significant due to the low energy region and the limited accessible *k*-range, therefore the values were constrained between 0.008–0.018 $Å^2$.

2) Second, an additional S–S scattering path was included in the models for which the fit qualities were found to be insufficient.

Acknowledgements

This work was supported by a Grant-in-Aid for Early-Career Scientists (No. 20K15027) from the Japan Society for the Promotion of Science (JSPS). The authors express their gratitude for funding by the German Research Foundation (Deutsche Forschungsgemeinschaft, DFG), Grant No. 398143140, related to the Research Unit FOR 2824 "Amorphous Molecular Materials with Extreme Non-Linear Optical Properties".

The S *K* and Sn L_3-edge experiments were performed at the beamline BL-11 in the HiSOR facility with the approval of the Hiroshima Synchrotron Radiation Center, Hiroshima University (Proposal Nos. 20AG034, 21AU003, and 21AG045). The Sn *K*-EXAFS measurements were performed at P65 of the PETRA III ring (Hamburg, Germany) with the Proposal No. I-20190122.

Conflict of Interest

The authors declare no conflict of interest.

Data Availability Statement

The data that support the findings of this study are available from the corresponding author upon reasonable request.

Keywords

amorphous compound, extended X-ray absorption fine structure spectroscopy, local structure, nonlinear optical properties, white-light generation, XANES

[1] N. W. Rosemann, J. P. Eussner, A. Beyer, S. W. Koch, K. Volz, S. Dehnen, S. Chatterjee, *Science* **2016**, *352*, 1301.
[2] N. W. Rosemann, J. P. Eußner, E. Dornsiepen, S. Chatterjee, S. Dehnen, *J. Am. Chem. Soc.* **2016**, *138*, 16224.
[3] S. Dehnen, P. R. Schreiner, S. Chatterjee, K. Volz, N. W. Rosemann, W.-C. Pilgrim, D. Mollenhauer, S. Sanna, *ChemPhotoChem* **2021**, *5*, 1033.
[4] I. Rojas-León, J. Christmann, S. Schwan, F. Ziese, S. Sanna, D. Mollenhauer, N. W. Rosemann, S. Dehnen, *Adv. Mater.* **2022**, *34*, 2203351.
[5] R. R. Alfano, *The Supercontinuum Laser Source*, Springer, New York **2016**.
[6] J. M. Dudley, G. Genty, S. Coen, *Rev. Mod. Phys.* **2006**, *78*, 1135.
[7] The NLO response of the η^1-Cp-cluster is somewhat controversial, as WLG was reported for it in ref. [8], but could not be reproduced in a recent attempt.[9] Still, it was argued that the cluster would be suitable for WLG from the structural point of view, but due to its low band gap energy, this process competes with a two-photon absorption process when irradiated with IR light, which leads to the destruction of the cluster during the optical measurement. Therefore, we keep its classification as a system with WLG here.
[8] E. Dornsiepen, F. Dobener, S. Chatterjee, S. Dehnen, *Angew. Chem., Int. Ed.* **2019**, *58*, 17041.
[9] J. Haust, J. Belz, M. Müller, B. D. Klee, J. L. Vasco, F. Hüppe, I. R. Léon, J. Christmann, A. Beyer, S. Dehnen, N. W. Rosemann, W.-C. Pilgrim, S. Chatterjee, K. Volz, *ChemPhotoChem* **2022**, *6*, 6.
[10] K. Hanau, S. Schwan, M. R. Schäfer, M. J. Müller, C. Dues, N. Rinn, S. Sanna, S. Chatterjee, D. Mollenhauer, S. Dehnen, *Angew. Chem., Int. Ed.* **2021**, *60*, 3.
[11] B. Klee, B. Paulus, J. L. Vasco, S. Hosokawa, J. Stellhorn, S. Hayakawa, S. Dehnen, W.-C. Pilgrim, *Scr. Mater.* **2022**, *219*, 114851.
[12] R. L. McGreevy, L. Pusztai, *Mol. Simul.* **1988**, *1*, 359.
[13] O. Gereben, L. Pusztai, *J. Comput. Chem.* **2012**, *33*, 2285.
[14] J. R. Stellhorn, S. Hayakawa, B. D. Klee, B. Paulus, J. L. Vasco, N. Rinn, I. R. León, S. Dehnen, W.-C. Pilgrim, *Phys. Status Solidi B* **2022**, *259*, 2200088.
[15] W.-C. Pilgrim, J. R. Stellhorn, B. D. Klee, J. L. Vasco, B. Paulus, A. Zeidler, S. Hosokawa, S. Hayakawa, S. Dehnen, *J. Phys. Soc. Jpn.* **2022**, *91*, 9.
[16] S. Gross, M. Bauer, *Adv. Funct. Mater.* **2010**, *20*, 4026.
[17] B. D. Klee, E. Dornsiepen, J. R. Stellhorn, B. Paulus, S. Hosokawa, S. Dehnen, W.-C. Pilgrim, *Phys. Status Solidi B* **2018**, *255*, 1800083.
[18] B. D. Klee, B. Paulus, S. Hosokawa, M. T. Wharmby, E. Dornsiepen, S. Dehnen, W.-C. Pilgrim, *J. Phys. Commun.* **2020**, *4*, 035004.
[19] D. Kobelt, E. F. Paulus, H. Scherer, *Acta Crystallogr., Sect. B: Struct. Crystallogr. Cryst. Chem.* **1972**, *28*, 2323.
[20] S. Hayakawa, Y. Hajima, S. Qiao, H. Namatame, T. Hirokawa, *Anal. Sci.* **2008**, *24*, 835.
[21] E. Welter, R. Chernikov, M. Herrmann, R. Nemausat, *AIP Conf. Proc.* **2019**, *2054*, 040002.
[22] B. Ravel, M. Newville, *J. Synchrotron Radiat.* **2005**, *12*, 537.